

# Beyond crossing fibres: Probabilistic tractography of complex subvoxel fibre geometries

Parya MamayezSiahkal<sup>†\*</sup>, Jennifer S. W. Campbell<sup>§†\*</sup>, Peter Savadjiev<sup>‡</sup>,  
G. Bruce Pike<sup>§</sup>, and Kaleem Siddiqi<sup>†</sup>

<sup>§</sup> McConnell Brain Imaging Centre, McGill University

<sup>†</sup> Centre for Intelligent Machines, McGill University

<sup>‡</sup> Brigham and Women’s Hospital, Harvard University

\*these authors contributed equally to this work

**Abstract.** Despite the development of different tractography schemes for reconstruction of fibre pathways, a comprehensive methodology that is capable of providing reliable uncertainty measures of the reconstructed tracts while exploring complex subvoxel fibre geometries, such as fanning, is still missing. In this article, we propose a probabilistic approach based on the residual bootstrap statistical technique, applied with detailed subvoxel geometry information obtained using a curve inference technique. We argue that the proposed framework can better represent the uncertainty due to noise in the fibre direction than the techniques that do not explicitly handle subvoxel fanning. This in turn leads to improvement in fibre tractography performance. We validate the performance of the algorithm with tractography in the human brain.

**Key words:** Diffusion MRI, Fibre orientation distribution, Tractography, Probabilistic labeling, Residual bootstrap, High angular resolution diffusion imaging, Fanning fibre, Curve inference

## 1 Introduction

Diffusion magnetic resonance imaging (DMRI) is the first noninvasive method capable of exploring neural connectivity and reconstructing white matter fibre structure *in vivo*. DMRI is able to probe white matter fibre orientation because water diffusion is anisotropic in brain white matter, leading to greater displacement of water molecules parallel to white matter fibre tracts. This characteristic can be used to reconstruct connectivity patterns between different cortical/subcortical areas of the brain. To do so, the first step in DMRI tractography is to estimate the diffusion probability distribution function (pdf) describing the anisotropic diffusion of water molecules in brain white matter. Several techniques have been developed to compute the diffusion pdf, ranging from diffusion tensor imaging (DTI) [1] which is a low angular resolution technique, to high angular resolution diffusion imaging (HARDI) techniques, such as diffusion spectrum

imaging (DSI) [2] and q-ball imaging (QBI) [3]. While DTI is the first successful technique in modeling the diffusion pdf, it fails to extract the true fibre structure within a voxel containing a crossing, branching or merging configuration of fibres due to its underlying assumption of a single anisotropic Gaussian pdf. Using the latter HARDI techniques, a diffusion orientation distribution function (ODF) can be obtained, which has the potential to model multiple fibre orientations within a voxel. More recent techniques have been developed for calculation of the fibre orientation distribution (FOD) [4, 5], which is the diffusion ODF deconvolved with a single fibre response function.

Regardless of the method used for the computation of diffusion ODFs or FODs, there are always uncertainties associated with the obtained fibre orientations. These uncertainties, which can be due either to acquisition noise or model deficiencies, should be incorporated in further processing, such as tractography, in order to represent the confidence in the reconstructed fibre pathways. To address this issue, there has been a wide body of research dedicated to probabilistic tractography. These probabilistic methods can be divided into two groups: those which model noise parameters by some probability distribution [6, 7] and bootstrap based methods which capture the uncertainty in the data by random selection from a set of different measurements [8, 9]. Probabilistic methods belonging to the first group essentially rely on an underlying noise model and prior distribution, and this may not always describe the actual uncertainties accurately. On the other hand, while traditional bootstrap methods can provide a nonparametric estimation of diffusion uncertainty, the need for multiple data acquisitions hinders any practical application of them to HARDI based techniques. A more practical alternative to the standard bootstrap method has been recently proposed, in the context of q-ball imaging, by Berman *et al.* [8], which requires only a single HARDI measurement.

It can be claimed that FODs obtained from HARDI measurements, combined with a bootstrap probabilistic approach, can characterize uncertainties in the fibre orientation to a good extent. Despite the significant improvement which can be expected using this technique, there still exist ambiguities in the subvoxel fibre structure which cannot be resolved by FODs [10]. An example of such failure is the discrimination between a fanning and curving fibre tract. In a recent work done by Savadjiev *et al.* [10], this issue has been addressed by implementing a 3D curve inference algorithm which assigns different labels to such ambiguous configurations. Improvement is shown in tractography using the curve inference labeling information, which differentiates among single, fanning and crossing fibre configurations.

We believe that FODs that have been postprocessed in a bootstrap probabilistic curve inference labeling framework would provide a better representation of fibre orientation and would certainly result in a more reliable reconstruction of connectivity patterns. In this paper, we combine bootstrap analysis of the FOD with the curve inference algorithm, in order to obtain uncertainties associated with the complex fibre configurations, including fanning. We then perform DMRI tractography using this entire pipeline, which allows us to define a confi-

dence value for each reconstructed tract. The results obtained validate our claim by showing improvement over other tractography methods that do not quantify uncertainty and/or take into account all possible subvoxel geometries.

## 2 Methods

### 2.1 Acquisition

MRI data were acquired for one healthy subject on a Siemens 3T Trio MR scanner (Siemens Medical Systems, Erlangen, Germany) using an 8-channel phased-array head coil. Diffusion encoding was achieved using a single-shot spin-echo echo planar sequence with twice-refocused balanced diffusion encoding gradients. A dataset designed for high angular resolution reconstruction was acquired with 99 diffusion encoding directions, 2mm isotropic voxel size, 63 slices,  $b=3000$  s/mm<sup>2</sup>, TE=121ms, TR=11.1s, and GRAPPA parallel reconstruction. A 1mm isotropic resolution T1 weighted anatomical scan was also acquired (TR=9.7ms, TE=4ms,  $\alpha=12^\circ$ ).

### 2.2 Probabilistic deconvolution

The diffusion weighted signal profiles were fitted to a spherical harmonic (SH) basis of order eight. Multiple (in this experiment, 100 iterations) diffusion weighted signal profiles were generated using the residual bootstrap, similar to approaches described previously for probabilistic q-ball imaging [8, 11]: For each iteration, the residuals from the SH fit of the original diffusion weighted signal profiles were added at random without replacement to the SH profile to generate a new diffusion weighted signal profile reflecting the noise characteristics of the acquisition. For each iteration, the new signal profile was input to a spherical deconvolution algorithm (an implementation of the approach of Anderson [4]). The deconvolved ODFs were used as input to a curve inference algorithm (an implementation of the approach of Savadjiev *et al.* [10]), which is described in the next section. The curve inference process labels the subvoxel fibre configuration for each iteration as either fanning, single, or multiple (i.e., crossing) curves, and gives the polarity of the fanning in the former case.

### 2.3 Curve inference algorithm: labeling of subvoxel fibre configurations

The 3D curve inference algorithm, developed by Savadjiev *et al.* [10, 12], exploits local differential geometry of 3D curves to infer the likely local curves modeled as helices. A co-helicity measure is defined to compute the degree of compatibility among triplets of orientations. Here, the curve inference algorithm is provided with FODs obtained from the deconvolution scheme described above. The inherent estimates of torsion and curvature, computed as part of the curve inference algorithm, are incorporated into a labeling framework in order to discriminate

between complex intravoxel fibre structures. Specifically, this algorithm allows for detection and description of subvoxel fanning. In this paper, *curve inference labeling* refers to this process of identifying voxels as containing fibres in one of several geometries including fanning. The following section describes how uncertainties are assigned to fanning fibres and other structures.

## 2.4 Probabilistic curve inference labeling

For each voxel in the diffusion MRI volume, the goal is to compute the confidence value of having fibres in a single, fanning or crossing fibre configuration, together with the corresponding cone of uncertainty around each fibre direction. To achieve this, as mentioned in section 2.3, the FOD computed at each iteration of the residual bootstrap algorithm is input to the curve inference labeling scheme. The outputs of the curve inference labeling algorithm are the labels assigned to each voxel and the corresponding fibre directions. In the cases of single or crossing fibres, these fibre directions are the FOD maxima. In the case of fanning, the output is two vectors representing the fanning extent, and a third vector representing its polarity. From the two fan delineating vectors, a 2D planar fan with a fan-shaped “cone” of uncertainty can be constructed, as described below. In this implementation, only crossings of up to three fibres are considered, as four way crossings were not detected with the angular and spatial resolution employed in the study. The vectors obtained from all iterations are matched and used to obtain mean vectors and standard deviations  $\sigma_\theta$  for these vector orientations for each configuration seen. Moreover, confidence values are computed at each voxel, reflecting the number of times a specific label has been assigned to that voxel. Fig. 1 shows the cone of uncertainty around each vector, where the vector is the mean for all iterations resulting in a given label, and the cone subtends the angle  $\sigma_\theta$  equal to the standard deviation of the orientations obtained. As a final step, the vectors obtained for each different configuration are matched to obtain an occurrence rate,  $O_v$ , of each *vector*. Specifically, if a vector is labeled as a single fibre direction on some iterations, and matches one of many crossing fibre directions on other iterations, and falls within a fan on other iterations, its occurrence will reflect all of these occurrences of this fibre direction. Hence, an occurrence  $O_v$  between 0 and 1 is assigned to each vector in each of four possible configurations: (a) single (potentially curving) fibre bundle, (b) double crossing, (c) triple crossing, and (d) fanning. In the case of curving, the tangent to the curve is output, and is used in tractography in a manner identical to that the case of a straight fibre.

## 2.5 Tractography

The tractography algorithm used was an extended streamline tracking algorithm implemented in a probabilistic framework which considers the probabilistic fibre orientation information obtained from the probabilistic curve inference labeling scheme. Here, the entire tractography process was run iteratively, with the direction of propagation chosen randomly using the output of the probabilistic

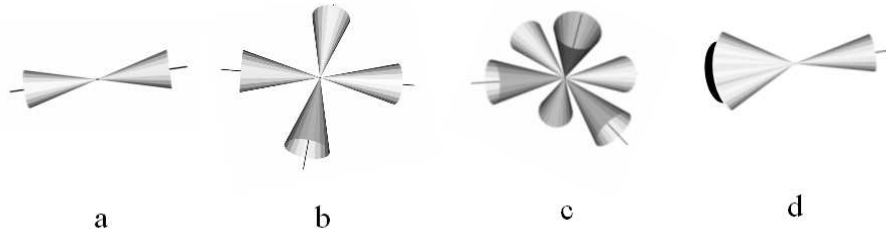


**Fig. 1.** Fibre configurations and cones of uncertainty obtained from the probabilistic curve inference labeling. The algorithm produces output for four possible configurations: (a) single (potentially curving) fibre bundle, (b) double crossing, (c) triple crossing, and (d) fanning fibres. In the case of fanning, fanning will occur in only one direction (to the left in this figure), while in the other direction, there is a merge.

curve inference labeling. Each time a direction of propagation,  $v_p$ , was chosen, an associated confidence value was assigned to it. As a first step in calculating a possible direction of propagation, for fibres in geometries (a) through (d) above, a fibre probability profile was generated. For geometries (a) through (c) (single and crossing fibres), and for the merge direction in geometry (d) (fanning), this fibre probability profile was generated for each fibre direction, and was given analytically by a truncated Gaussian distribution centred at the mean fibre direction, with standard deviation  $\sigma_\theta$  for that direction obtained from the bootstrap deconvolution, and truncated at one standard deviation from the mean. On each iteration in tractography, the vector  $v_p$  was selected at random from within this probability profile, and the confidence value for this vector was given by the value of this truncated Gaussian in the direction of  $v_p$ . For the fanning direction in geometry (d), the probability profile was defined as shown in Fig. 2, as a fan-shaped “cone” that takes into account the potentially different  $\sigma_\theta$  values for the two fan delineating vectors  $v_{o_{1,2}}$  output by the curve inference. The direction of propagation  $v_p$  was chosen at random from within this cone. The probability profile value in direction  $v_p$  subtending angle  $\theta$  with the plane segment subtended by vectors  $v_{o_{1,2}}$  (dashed line in Fig. 2) was given by the value of a Gaussian distribution with mean zero and standard deviation determined by the weighted average of the standard deviations for the vectors  $v_{o_{1,2}}$ , with weights determined by the proximity of  $v_p$  to the vectors  $v_{o_{1,2}}$ . If  $v_p$  was further away from  $v_{o_2}$  than was  $v_{o_1}$ , then the standard deviation for  $v_{o_1}$  was used. The confidence value for the vector was given by the value of this Gaussian-based probability profile. Note that this process means that the confidence value for *all* vectors that lie on the 2D planar fan subtended by  $v_{o_{1,2}}$  is high, and that the confidence values only fall off lateral to this fan and distal to the end vectors. Note also that because the two fan-delineating vectors both have uncertainty,

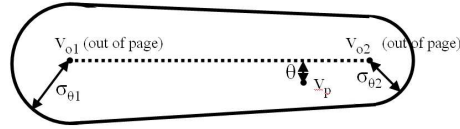


**Fig. 2.** View of the top edge of the cone of uncertainty for the fanning fibre configuration. The two fan-delineating vectors  $v_{o_{1,2}}$  point out of the page and have associated angular standard deviations  $\sigma_{\theta_{1,2}}$ . The circular ends of the cones of uncertainty around each of these vectors are joined by tangent straight lines, and the direction of propagation for tractography ( $v_p$ ) is chosen from within the solid line. Its confidence value is given by a Gaussian evaluated at angle  $\theta$  subtended by  $v_p$  and the planar segment (whose edge is the dotted line) subtended by  $v_{o_{1,2}}$  (see text for details).

both the orientation and the extent of the fan vary with iteration. Fig. 3 shows schematic fibre probability profiles for single and crossing fibres.

Given the above probability profiles for each possible fibre configuration at each voxel, the tractography proceeded as follows. Streamlines were iteratively propagated using Fibre Assignment by Continuous Tracking (FACT) integration [13]. For each iteration, at each voxel reached, one fibre geometry was chosen at random from all geometries with nonzero occurrence. Next, one fibre direction (or fan in the case of fanning) was chosen for this geometry. In the case of crossing fibres, the direction closest to the incoming direction was chosen. In the case of fanning, the merge direction was chosen if the dot product between the incoming direction and the polarity vector was negative, otherwise, fanning was chosen. Next, a vector from within the chosen fibre direction’s probability profile was chosen at random and its confidence value, described above, was saved. The confidence value for this vector tract segment was then scaled by the occurrence rate  $O_v$  for the selected fibre. As the iterative tractography process evolved, confidence values were assigned to the streamlines using a *weakest link* approach [14–16]: the confidence in a given streamline is given by the lowest confidence value of all tract segments along the streamline. The connectivity index for each voxel in the imaging volume to a given reference region of interest (ROI) was then assigned. The connectivity index for voxel B to the reference ROI is given by the highest confidence value over all the streamlines connecting voxels in the reference ROI to voxel B. Fig. 3 illustrates this *weakest link* connectivity approach.

Several tractography experiments were run. For each of three seed ROIs, tracking was done using (a) curve inference labeling of subvoxel geometries, but no probabilistic framework, i.e., no bootstrapping was performed, but the labeling was run once on the original data, (b) bootstrap probabilistic framework, but no curve inference, i.e., no treatment of fanning fibres, and (c) both (i) probability profiles generated using the residual bootstrap and (ii) curve inference

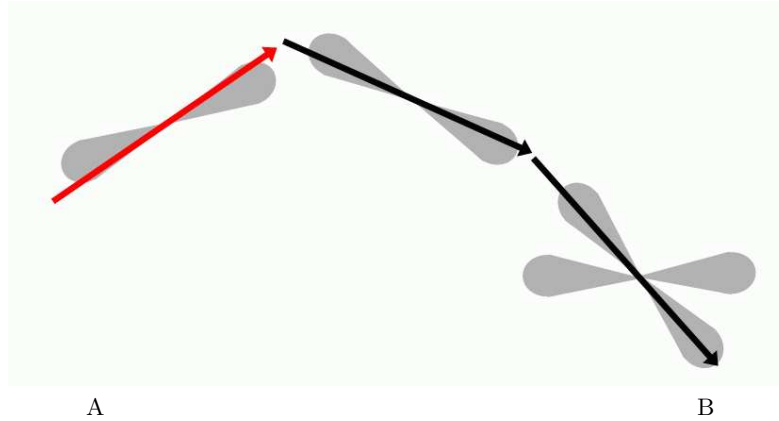


**Fig. 3.** Truncated Gaussian fibre probability profiles, shown in 2D for illustration. The tractography process propagates streamlines iteratively with the direction of propagation chosen from within the truncated Gaussian cones of uncertainty. The confidence in this tract segment generated is given by the scaled value of the truncated Gaussian in the direction propagated. The confidence value for a streamline connecting voxel B to voxel A is given by the lowest confidence value for all segments along that streamline. Here, the red tract segment is that with lowest confidence. The scalar connectivity index for connection of voxel B to reference voxel A will be given by the maximal confidence value of all streamlines that connect the two voxels.

labeling of subvoxel geometries including fanning. In case (b), note that all fibre directions for all geometries are still assigned the occurrence  $O_v$ , but the fanning geometry is not considered. Table 1 summarizes the processing for the combined curve inference labeling and bootstrap probabilistic pipeline (c).

The three ROIs used were placed in (1) the medial genu of the corpus callosum, (2) the medial corpus callosum at the level of the premotor cortex, and (3) the internal capsule. 1000 iterations of the probabilistic tractography were run for all seed ROIs. For all seed ROI voxels, the tracking was initiated on a  $3 \times 3 \times 3$  grid of start points in order to facilitate branching. The tracking was stopped if the fractional anisotropy (FA) was less than 0.1, the mean diffusivity was greater than  $1.0^{-6} \text{mm}^2/\text{ms}$ , or the turning angle from one voxel to the next was greater than  $70^\circ$ . For the second ROI in the corpus callosum, tracts that erroneously turned down the cortical-spinal tract were excluded. Connectivity index maps were stored for all experiments, with the connectivity index reflecting the confidence in connection of each voxel in the volume to the seed ROI.

### 3 Results

Fig. 4 shows the computed mean fibre directions and cones of uncertainty for the four different fibre configurations in a small ROI in the brain. There is

- acquire high angular resolution diffusion weighted signal profile
- fit signal profile to SH basis
- For  $N$  iterations
  - {
  - perform residual bootstrap generation of synthetic signal profile by adding residuals at random to SH fit of original
  - perform spherical deconvolution to calculate FOD
  - perform curve inference labeling on FOD to obtain fibre geometry labels and fibre directions
  - }
- calculate mean, standard deviation ( $\sigma_\theta$ ), and occurrence ( $O_v$ ) of each fibre direction, including fan delineating vectors, from the combined output of the  $N$  iterations.
- run iterative probabilistic tractography

**Table 1.** Summary of the data processing pipeline for the combined curve inference labeling and bootstrap probabilistic tractography. In this study, the number of bootstrap iterations  $N=100$ .

output at each voxel for each fibre configuration that has greater than zero occurrence, hence, all four geometries may be shown at a given voxel, despite some geometries being relatively insignificant. Fig. 5 shows the results of the tracking experiments. On the left in (a) is the tracking result using curve inference labeling of fanning fibres, but no probabilistic framework. At centre (b) is the result using the bootstrap probabilistic framework but no curve inference labeling. The result using both (i) the bootstrap probabilistic approach and (ii) curve inference labeling is shown at right in (c).

## 4 Discussion

The tractography results presented in the previous section affirm the potential of the proposed probabilistic curve inference labeling tractography pipeline to describe fibre pathways that pass through regions of complex subvoxel geometries, including subvoxel fanning. Whereas most fibre tracking algorithms provide reasonable results in major fibre tracts, incorporation of uncertainties obtained from a probabilistic scheme can improve the result of tractography by following fibre pathways closer to the cortex, where the fibre directional uncertainty is higher due to more complex fibre structures. Moreover, the curve inference labeling algorithm incorporated into a probabilistic framework can help to obtain more accurate confidence indices in tractography by exploring the ambiguities in the FOD, and expanding on the single or crossing fibre subvoxel geometry assumption.

For all of the tracking experiments performed, it is clear that the results obtained by using probability profiles (columns (b) and (c) of Fig. 5) are generally much more extensive than the non-probabilistic approach (column (a)), as ex-

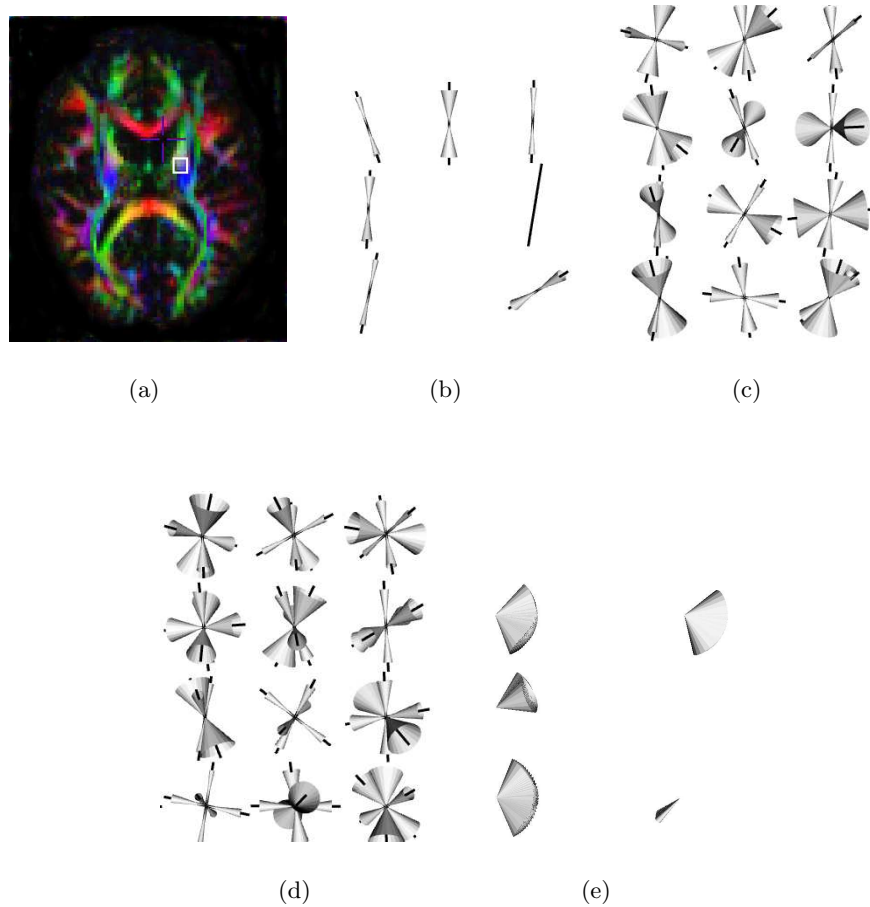


**Fig. 4.** Cones of uncertainty in a small ROI for the four configurations: (b) single fibre direction; (c) double crossing; (d) triple crossing; (e) fanning fibres. For (b)-(e), the data are shown in the same ROI: the cones are shown wherever a configuration has greater than zero occurrence, hence, at any given voxel there could be up to four fibre configurations shown here. The ROI used is marked by a white square on the principal diffusion direction red-green-blue (RGB) image (a). In the RGB image, red represents left-right orientation, green represents anterior-posterior orientation and blue represents inferior-superior orientation.

pected. There are places, however, where non-probabilistic fanning (a) results in connectivity to regions that are not reached with the probabilistic non-fanning approach (b), as can be seen in the leftmost lateral corpus callosum connections in the top two rows of Fig. 5. This is expected, because the cones of uncertainty for single fibres in (b) would not be expected to be as broad as fannings could

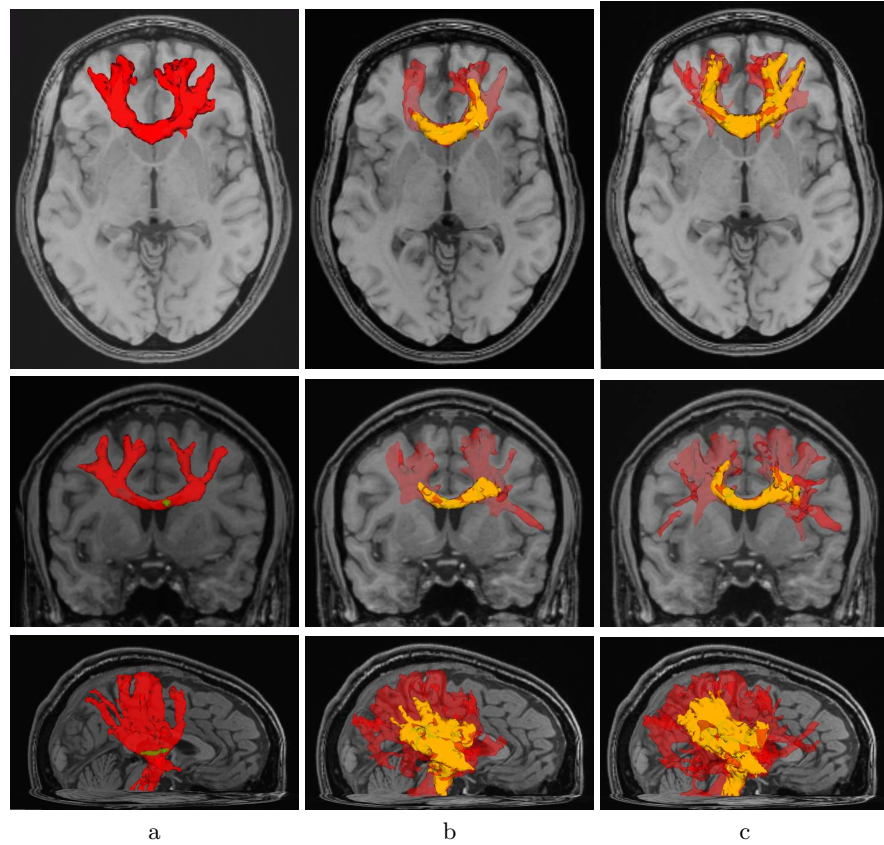


**Fig. 5.** Fibre tractography results in the human brain. (a) Tracking with curve inference labeling, no probabilistic framework; (b) bootstrap probabilistic framework, no curve inference labeling; (c) curve inference labeling and bootstrap probabilistic framework. The results in (b) and (c) are shown as two surfaces encompassing two level sets of the connectivity index map, shown in red and yellow. The translucent red surface is that encompassing the lowest non-zero connectivity index values. Note that the surface shown in column (a) is simply the full extent of all voxels reached in the deterministic scheme: there is no connectivity index information in this scheme. The top row is the result using the starting ROI in the genu of the corpus callosum, the middle row is the result using the starting ROI in the corpus callosum at the level of premotor cortex, and the bottom row is the result using the internal capsule starting ROI.

be in (a), and hence would not result in projections to as many voxels. The results of the probabilistic approach excluding fanning information are always a subset of those which incorporate labeling of fanning, as expected, because the act of fanning reaches a wider area. The difference in overall extent of the tractography result between non-probabilistic and probabilistic schemes is generally,

but not always, more marked than that between probabilistic frameworks with and without curve inference labeling, i.e., the difference between using fanning and not using fanning is often subtle, while many connections can be lost when tracking only along the most certain directions at each voxel.

For the corpus callosum seed ROIs, the highest connectivity values occur in the medial core of the corpus callosum, where the voxels are expected to contain large volume fractions of single fibre directions. This is expected given that the reproducibility of single fibre directions was seen to be high. The connectivity index then drops near the cortex, where fibre directional coherence drops, and there is more partial volume averaging of fibres with other fibre populations and with grey matter and cerebral spinal fluid.

When comparing the results of the three tractography schemes, it is important to note that the voxels reached without incorporating the probability profiles (column (a)) are not necessarily those assigned high connectivity indices in the probabilistic scheme. This observation is explained by the fact that if  $\sigma_\theta$  is high, even the tract segments that pass along the maximum of the Gaussian probability profile will be assigned lower confidence values than those tract segments that pass near, but not exactly along, a maximum in voxels with low  $\sigma_\theta$ . Also, the tracking results in lower connectivity indices in many places when fanning is ignored. For example, comparing columns (b) and (c), the high connectivity index region extends further out of the medial core of the fibre pathways shown. This is expected because while these voxels were reached in both experiments, in the case of probabilistic curve inference labeling, they were reached by propagating within the fan, where all confidence values are high. But without curve inference labeling information, the same voxels were reached by propagating near the edge of the cone of uncertainty for a single fibre, where the confidence values are low.

More experimental work is required to assess the validity and reproducibility of the proposed framework. In future work, we are planning to acquire multiple HARDI measurements and compare the above estimated uncertainties with the actual measured values. Running more iterations of the residual bootstrap scheme and comparing to other probabilistic methodologies are further issues to be addressed. Nevertheless, we believe that the results obtained thus far are encouraging and demonstrate the potential of this new approach.

## References

1. P.J. Basser, J. Mattiello, and D. Le Bihan. MR diffusion tensor spectroscopy and imaging. *Biophysical Journal*, 66:259–267, January 1994.
2. D.S. Tuch, M.R. Wiegell, T.G. Reese, J.W. Belliveau, and V. Wedeen. Measuring cortico-cortical connectivity matrices with diffusion spectrum imaging. In *Proceedings of International Society of Magnetic Resonance in Medicine*, page 502, Glasgow, Scotland, April 2001.
3. David S. Tuch. Q-ball imaging. *Magn. Reson. Med.*, 52:1358–1372, December 2004.
4. A.W. Anderson. Measurement of fiber orientation distributions using high angular resolution diffusion imaging. *Magnetic Resonance in Medicine*, 54(5):1194–1206, 2005.

5. J.D. Tournier, F. Calamante, D.G. Gadian, and A. Connelly. Direct estimation of the fiber orientation density function from diffusion-weighted MRI data using spherical deconvolution. *NeuroImage*, 23:1176–1185, September 2004.
6. G.J.M. Parker and D.C. Alexander. Probabilistic Monte Carlo based mapping of cerebral connections utilising whole-brain crossing fibre information. In *Proceedings of IPMI*, pages 684–695, Ambleside, UK, jul 2003.
7. T.E. Behrens. Probabilistic diffusion tractography with multiple fibre orientations: what can we gain? *NeuroImage*, 34:144–155, 2007.
8. J.I. Berman, S. Chung, P. Mukherjee, C.P. Hess, E.T. Han, and R.G. Henry. Probabilistic streamline q-ball tractography using the residual bootstrap. *NeuroImage*, 39(1):215–222, 2008.
9. D.K. Jones and C. Pierpaoli. Confidence mapping in diffusion tensor magnetic resonance imaging tractography using a bootstrap approach. *Magn. Reson. Med.*, 53:1143–1149, 2005.
10. P. Savadjiev, J. S. Campbell, G. B. Pike, and K. Siddiqi. Labeling of ambiguous sub-voxel fibre bundle configurations in high angular resolution diffusion MRI. *NeuroImage*, 41(1):58–68, 2008.
11. H. Haroon and G. Parker. Using variants of the wild bootstrap to quantify uncertainty in fibre orientations from q-ball analysis. In *Proceedings of the 2007 Organization for Human Brain Mapping annual meeting*, page 273, 2007.
12. P. Savadjiev, J.S. Campbell, and B.G. Pike K. Siddiqi. 3d curve inference for diffusion MRI regularization and fibre tractography. *Med. Image Anal.*, 10:799–813, August 2006.
13. S. Mori, B.J. Crain, VP. Chacko, and P.C.M. van Zijl. Three dimensional tracking of axonal projections in the brain by magnetic resonance imaging. *Annals of Neurology*, 45:265–269, 1999.
14. C. Lenglet, J.S.W. Campbell, M. Descoteaux, Haro G., P. Savadjiev, D. Wassermann, A. Anwender, R. Deriche, G.B. Pike, G. Sapiro, K. Siddiqi, and P Thompson. Mathematical methods for diffusion MRI processing. *NeuroImage*, 45(1 Suppl):S111–22, 2008.
15. G.J.M. Parker, C.A.M. Wheeler-Kingshott, and G.J. Barker. Estimating distributed anatomical connectivity using fast marching methods and diffusion tensor imaging. *IEEE Transactions on Medical Imaging*, 21(5):505–512, 2002.
16. J.S.W. Campbell, K. Siddiqi, V.V. Rymar, A.F. Sadikot, and G.B. Pike. Flow-based fiber tracking with diffusion tensor and q-ball data: Validation and comparison to principal diffusion direction techniques. *NeuroImage*, 27(4):725–736, October 2005.